Interaction of Antimicrobial Peptides with Lipopolysaccharides†

Lai Ding,‡ Lin Yang,‡,§ Thomas M. Weiss,‡,|| Alan J. Waring,⊥,# Robert I. Lehrer,⊥ and Huey W. Huang*,‡

Department of Physics and Astronomy, Rice University, Houston, Texas 77251-1892, and Departments of Medicine and Pediatrics, University of California−Los Angeles School of Medicine, Los Angeles, California 90095

Received July 1, 2003; Revised Manuscript Received September 3, 2003

ABSTRACT: We study the interaction of antimicrobial peptides with lipopolysaccharide (LPS) bilayers to understand how antimicrobial peptides interact with the LPS monolayer on the outer membrane of Gram-negative bacteria. LPS in water spontaneously forms a multilamellar structure composed of symmetric bilayers. We performed X-ray lamellar diffraction and wide-angle in-plane scattering to study the physical characteristics of LPS multilayers. The multilayer alignment of LPS is comparable to phospholipids. Thus, it is suitable for the application of oriented circular dichroism (OCD) to study the state of peptides in LPS bilayers. At high hydration levels, the chain melting temperature in multilamella detected by X-ray diffraction is the same as that of LPS aqueous dispersions, as measured by calorimetry. LPS has a strong CD, but with a careful subtraction of the lipid background, the OCD of peptides in LPS is measurable. The method was tested successfully with melittin. It was then applied to two representative antimicrobial peptides, magainin and protegrin. At peptide concentrations comparable to the physiological conditions, both peptides penetrate transmembrane in LPS bilayers. The results imply that antimicrobial peptides readily penetrate the LPS monolayer of the outer membrane.

Gram-positive bacteria are typically surrounded by a thick and mechanically strong peptidoglycan cell wall whose coarse meshwork offers little resistance to the diffusion of small molecules such as antibiotics (*1*). In contrast, the cytoplasmic membrane of Gram-negative bacteria is enveloped by two structures, a thin peptidoglycan wall that is surrounded by a highly asymmetrical membrane bilayer called the outer membrane. The inner leaflet of the outer membrane is composed of phospholipids resembling those of the cytoplasmic membrane, but its outer leaflet is composed mostly of lipopolysaccharide (LPS)[1] (*2*). Because this outer leaflet is a barrier to the passage of many molecules, the outer membrane contains proteins called porins that form aqueous transmembrane diffusion channels. Those of *Escherichia coli* are believed to freely allow the passage of hydrophilic solutes up to 600 Da. The question concerning us here is the following: how do antimicrobial peptides (typically >2000 Da) whose ultimate target is the cytoplasmic membrane pass through the outer membrane?

LPS is a unique constituent of the bacterial outer membrane. It is composed of three parts: the proximal, hydrophobic lipid A region; the distal, hydrophilic, O antigen polysaccharide region that protrudes into the medium; and the core oligosaccharide region that connects the two (*2*). Lipid A is a disaccharide of glucosamine attached to six or seven fatty acid residues, some hydroxylated but all of them saturated. The proximal part of the core and the lipid A backbone contain a large number of charged groups, most of them anionic. Various mutants produce LPS molecules without O antigen and part of the core, as in the deep rough mutants (i.e., the Rd_1, Rd_2, and Re chemotypes; see ref *2*). These simpler LPS (i.e., the Rd and Re chemotypes) will be used in this first study with antimicrobial peptides. Snyder and McIntosh studied antibiotic permeability to these LPSs (*3*).

Gene-encoded antimicrobial peptides are ubiquitous components of host defense systems in animals and plants (*4*−*6*). Accumulated evidence strongly suggests that most of these peptides act by permeabilizing the cell membranes of microorganisms (see reviews in ref *7*). Thus, the peptide interactions with membranes have been a subject of active research recently. The standard method for such studies has been using model membranes made of phospholipids (see reviews in refs *8* and *9*) that were intended to mimic the lipid matrixes of plasma membranes. However, corresponding studies with the outer membranes of Gram-negative bacteria are yet to be undertaken. One obstacle has been the lack of convenient models for the outer membranes since it can be difficult to prepare an asymmetric model membrane. The unique characteristic of the outer membrane is the LPS monolayer. Our idea here is to probe the properties of the LPS monolayer by a study of LPS bilayers.

† H.W.H. was supported by NIH Grants GM55203 and RR14812 and by the Robert A. Welch Foundation. R.I.L. was supported by NIH Grants AI-22839 and AI37945.

* To whom correspondence should be addressed. Telephone: (713) 348-4899. Fax: (713) 348-4150. E-mail: hwhuang@rice.edu.

‡ Rice University.

§ Current address: National Synchrotron Light Source, Brookhaven National Laboratory, Upton, NY 11973.

|| Current address: High Brilliance Beamline ID02, European Synchrotron Radiation Facility, 6, Rue Jules Horowitz BP220, F-38043 Grenoble Cedex 9, France.

⊥ Department of Medicine, UCLA School of Medicine.

Department of Pediatrics, UCLA School of Medicine.

[1] Abbreviations: LPS, lipopolysaccharide; EDTA, ethylenediaminetetraacetic acid; OCD, oriented circular dichroism; P/L, peptide-to-lipid molar ratio; DMPC, dimyristoyl phosphatidylcholine; DLPC, dilauroyl phosphatidylcholine; DPhPC, diphytanoyl phosphatidylcholine; DOPC, dioleoyl phosphadylcholine; POPC, palmitoyl-oleoyl phosphatidylcholine.

10.1021/bi035130+ CCC: $25.00
Published on Web 10/03/2003

Experiments have shown that some properties of a bilayer are the sum of that of the two leaflets. In some instances, individual leaflets of membrane bilayers could alter their physical properties independent of the other leaflet. Zeidel and collaborators (*10*, *11*) made asymmetric bilayers by adding cholesterol sulfate or Pr^{3+} to one leaflet and measured the permeabilities to water, glycerol, formamide, and acetamide. Their results showed that each leaflet exerts an independent resistance to the passage of solutes, such that the overall permeability (P_{ab}) is the inverse of the sum of resistances given by two leaflets: $1/P_{ab} = (1/P_a + 1/P_b)$. Thus, it was suggested that cells create apical membranes of low permeability by segregating phospholipid molecules with long saturated hydrocarbon chains and cholesterol in the outer leaflet of the bilayer. By this argument, an LPS bilayer has twice the effect of resistance to antimicrobial peptides as that of an LPS monolayer. To the extent that we are trying to understand the interactions of antimicrobial peptides with LPS monolayers, it is reasonable to expect useful information from a study of the interactions between peptides and LPS bilayers.

The pioneer biophysical studies of LPS by investigators such as Labischinski et al. (*12*), Kastowsky et al. (*13*), Snyder et al. (*14*), and Snyder and McIntosh (*3*) have shown that LPS molecules spontaneously form symmetric bilayers in aqueous solution. We used oriented multiple bilayers of LPS for this study and examined the physical state of LPS bilayers by X-ray diffraction. We found that in full hydration, the bilayers in oriented multilamellae have the same properties as LPS bilayers in the vesicular form, having the same gel-to-fluid transition temperature and similar undulation fluctuations.

We then used the method of oriented circular dichroism (OCD) (*15*, *16*) to study the orientation of antimicrobial peptides in LPS bilayers. This was the method that discovered peptides changing orientation as a function of peptide concentration in phospholipid bilayers (*17*). We found that the application of OCD to peptides in LPS requires extra care because of the strong CD of LPS itself. The application was first tested with the well-studied membrane-active peptide melittin. We found that the OCD spectra of melittin were the same as those obtained in phospholipid bilayers, and melittin also changes orientation in LPS bilayers as a function of the peptide concentration just like in phospholipid bilayers.

To study the LPS interaction with antimicrobial peptides, we selected two representative peptides, one α-helical and one β-sheet, and each is the best-studied of its kind. Magainin-2 is a 23-residue peptide secreted by the skin of the African clawed frog *Xenopus laevis* (*18*). It dissolves in aqueous solution in a random coil form but assumes an α-helical conformation upon binding to a lipid bilayer. Protegrin-1 is an 18-residue peptide isolated from the leukocytes of pigs (*19*). Its native form in aqueous solution is a one-turn β-hairpin stabilized by two disulfide bonds, and the conformation is unchanged when bound to a lipid bilayer. Both peptides have been studied extensively, and their interactions with phospholipid bilayers are largely understood (see references in ref *9*). In the following study, we found that both peptides readily penetrate LPS bilayers.

MATERIALS AND METHODS

Materials. LPS from *Salmonella minnesota* strain R7 (Rd1 mutant) and strain R595 (Re mutant) were purchased from Sigma Chemical Co. (St. Louis, MO). The chemical structures of these chemotypes were described in ref *2*. Melittin was purchased from Sigma-Aldrich Chemical Co. (St. Louis, MO). Magainin-2 amide was a gift from Drs. Michael Zasloff and W. Lee Maloy of Magainin Pharmaceuticals Inc. (Plymouth Meeting, PA). Protegrin-1 was a gift from Dr. John Fiddes of IntraBiotics Pharmaceuticals, Inc. (Mountain View, CA). Silicon (001) wafers were purchased from Semicondutor Processing (Boston, MA). All materials were used as delivered.

Oriented Multilamellar Samples. We followed a previously described EDTA/HCl washing procedure to ensure that LPS was in a single, defined salt form (*3*). Briefly, (a) the purchased LPS powder was dissolved in a solution of triethylammonium EDTA (pH 7.0), sonicated for about 20 min to a clear solution. (b) The solution was extracted with 2.5 volumes of 2:1 chloroform/methanol. The extracted solution was vortexed and centrifuged for about 30 min to obtain a clear separation of the aqueous (upper) and organic (lower) phases. (c) The organic phase was transferred to a fresh bottle of 0.4 volume of methanol and 0.6 volume of 0.1 N HCl and vortexed and centrifuged as in step b. (d) The aqueous phases of both steps b and c were subsequently processed by the same centrifuge procedure. (e) The organic phases from steps c and d were combined together and dried under nitrogen gas. After adding a proper amount of water, the solution was sonicated for about 15 min. The LPS suspension was ready to use.

For LPS samples including ions (Ba^{2+}, Ca^{2+}, Mg^{2+}, Na^{+}), chloride or acetate salt solutions were added to the LPS suspension at the chosen ion-to-lipid ratio and vortexed for several minutes. Similarly peptides were added to the LPS suspension at the desired peptide-to-lipid ratio. The mixture was then vortexed and sonicated for 20 min.

The silicon wafers were cleansed with a 1:1 chloroform/methanol solution in an ultrasound cleaner and rinsed thoroughly with ethanol. To prepare an oriented multilayer sample, several drops of the LPS suspension were deposited on a clean silicon substrate. The sample was kept at 35 °C in an oven to let the water evaporate. While the water evaporated, LPS molecules self-assembled into parallel multiple layers of lipid bilayers intercalated with thin layers of water, as will be proven by X-ray diffraction experiments described next. Subjecting the sample to hydration cycles with the relative humidity (RH) varying between 65 and 100% RH and temperature cycles between 25 and 60° usually improved the alignment. Besides proving that LPS formed bilayers, X-ray diffraction was also used to inspect the degree of multilayer alignment (which was important for the measurement of peptide orientation) and the physical state of the lipid (i.e., whether the lipid was in the fluid or the gel state).

X-ray Diffraction. The sample was placed in a temperature-humidity chamber with Mylar windows for the passage of the X-ray, as described in Yang et al. (*20*). X-ray diffraction was conducted on a Huber four-circle goniometer, with a line-focused (10 mm vertical × 1 mm horizontal) CuK_α (wavelength 1.54 Å) source operating at 40 kV and 35 mA.

At a 6° takeoff angle (the projected source dimension 10 × 0.1 mm^2), the incident beam was collimated by a horizontal soller slit and two vertical slits on the front and the back sides of the soller slit. The horizontal and vertical divergences of the incident beam were 0.23 and 0.4°, respectively. The diffracted beam first passed through a vertical slit and then was discriminated by a bent graphite monochromator before entering a scintillation detector that was biased to discriminate against higher harmonics. A diffracted beam monochromator has the advantage over an incident beam monochromator in that the Compton scattering and the fluorescence from the sample are screened; consequently, the background signal is greatly reduced, which in turn allows the measurement of high diffraction orders.

The substrate of the sample was aligned carefully with respect to the incident X-ray beam (*21*). At a Bragg peak, a two-dimensional (ω, 2θ) scan was recorded to examine the quality of the sample. (ω is the incident angle with the plane of membranes, and 2θ is the total scattering angle.)

Samples of good quality were scanned by the $\omega - 2\theta$ process from $\omega = 0.5$ to ~8° with the step size $\Delta\omega = 0.02°$, repeated about every hour. At each temperature, the sample was scanned through a series of humidity levels ranging from RH ~75 to ~100%. The relaxation time to a new humidity setting varied. The hydration condition of the sample was considered to be in equilibrium if four consecutive scans produced the same pattern within a few percent. The four scans were then averaged to create one diffraction pattern for analysis.

The procedure for data reduction has been described in detail in previous publications (*21*−*23*). Briefly, it consisted of the following steps. A background curve was generated by removing all of the Bragg peaks from all of the data sets of a particular sample and then averaging the results and interpolating over any remaining gaps. After the background removal, a correction for the sample size versus the beam size (i.e., the diffraction volume) together with the absorption correction was carried out for each data point. Each Bragg peak was then fit with a Gaussian and integrated to obtain the intensity of that order. The integrated intensity was corrected for the polarization and the Lorentz factors. The square root of the integrated intensity is the relative magnitude of the scattering amplitude. The phasing diagrams were constructed by the Blaurock method (*24*). With the phases determined, the relative scattering amplitudes were Fourier transformed to produce unnormalized electron density profiles $\rho(z)$, where z is the coordinate normal to the plane of membranes.

X-ray In-Plane Scattering. For in-plane scattering (*25*, *26*), a point source of CuK$_\alpha$ radiation was used. After a thin Ni filter removed most of the CuK$_\beta$ radiation, the beam was focused by a pair of spherically bent mirrors (Charles Supper Co. Natick, MA). X-ray scattering was recorded on a Siemens X1000 multiwire proportional chamber (512 × 512 pixel; Bruker AXS Inc., Madison, WI) at the sample-to-detector distance of 25.01 cm. The distance was measured by using sucrose powder as a calibration standard. A helium path filled the space between the sample and the detector. The multilayer sample was oriented at a grazing angle.

Oriented Circular Dichroism. Oriented circular dichroism (OCD) is a simple method for detecting the orientation of peptides embedded in lipid bilayers using a conventional CD machine (*15*, *16*). A Jasco J-500A spectropolarimeter was used for this experiment. The procedure of OCD measurement is the same as the conventional CD measurement except that an oriented sample is used. For most experiments as in this one, normal (rather than oblique) incidence OCD is sufficient for the orientation analysis (*16*). OCD has been used to determine the orientation of various helical peptides including alamethicin (*15*−*17*, *27*), magainin (*28*), melittin (*29*) and synthetic helices (*30*), β-sheet peptides protegrins (*31*), and cyclic peptides θ-defensins (*32*). LPS bilayers have a strong OCD. Thus, for each measurement of a peptide in LPS, the corresponding pure LPS spectrum was measured for the purpose of background removal.

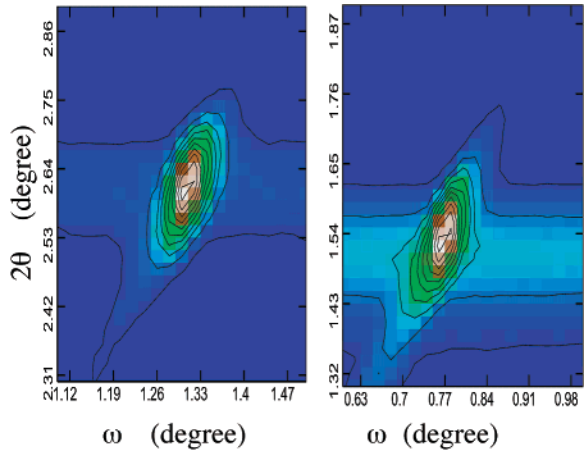

FIGURE 1: Two-dimensional (ω, 2θ) scan by X-ray of a LPS Rd multilayer sample around the second Bragg peak (left) and of a LPS Re containing protegrin-1 at P/L = 1:10 around the first-order Bragg peak (right).

RESULTS AND DISCUSSION

Rd-LPS and Re-LPS. All measurements were done with both LPS Rd and LPS Re. The results were very similar between them. In the following, LPS refers to both LPS Rd and LPS Re, unless the chemotype is specified.

State of LPS Multilayers. We will first characterize, by X-ray diffraction, the physical state of LPS with which the antimicrobial peptides interact. An important precondition for both the X-ray and the OCD experiments was to show that the multilayers were well-aligned. Figure 1 shows two examples of the two-dimensional (ω, 2θ) scan around a Bragg peak, one for a pure LPS sample and another for LPS containing protegrin at P/L = 1:10. At a small incident angle, the incident beam covered a large area of the sample (44 mm^2 at ω ~1.3° and 74 mm^2 at ω ~0.77°). Within this area, there was only one peak. The small mosaic spread, FWHM (the full width at half the maximum) ~0.06°, shows that the majority of LPS formed well-aligned multilayers. The low intensity band extended on both sides of the peak along the ω axis is the diffraction from the misaligned part of the sample. This band usually extended to 1−1.5° on each side (*33*), indicating that a minority of LPS were multilamella misaligned within ~1.5°. This minority part did not contribute to the diffraction analysis but was included in the OCD measurement. In general, OCD is not sensitive to the peptide orientation within a few degrees (*16*). The OCD spectra shown below also indicated that the whole samples were aligned within a few degrees.

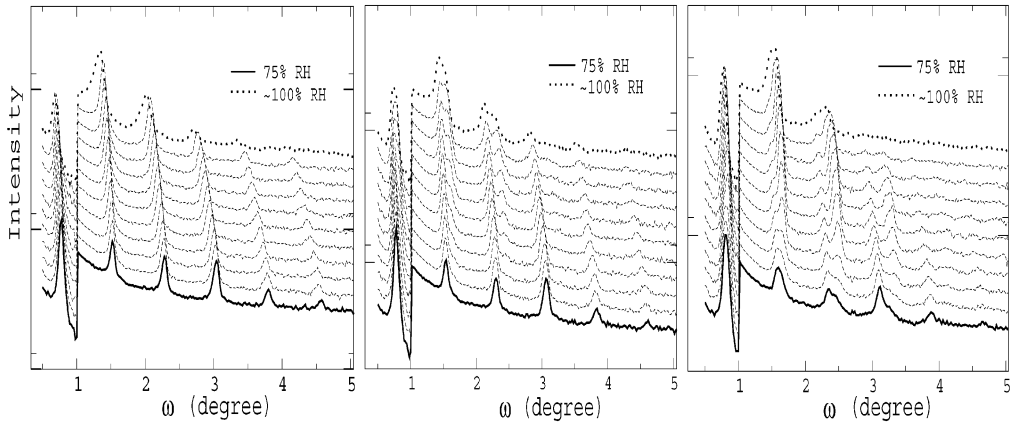

FIGURE 2: X-ray diffraction patterns of an LPS Re multilayer sample at three different temperatures, 25 °C (left), 35 °C (middle), and 40 °C (right), as the hydration level increased from 75% RH (bottom curve) to ~100% RH (top curve). Below $\omega = 1°$, an X-ray attenuator was used so as not to saturate the photon counter.

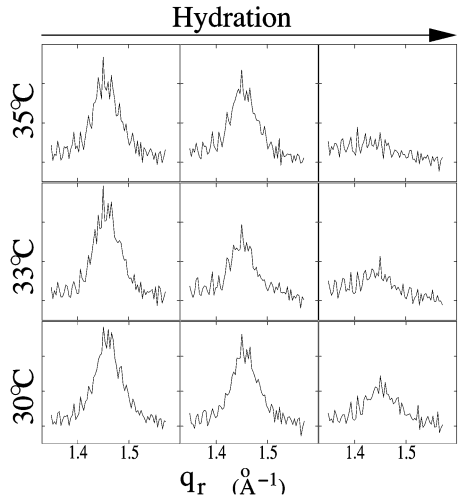

FIGURE 3: X-ray in-plane scattering of a LPS Rd multilayer sample at three different temperatures as the hydration level increased from left to right: 85% RH for the left column, 90% RH for the middle column, and ~96% RH for the right column. RH higher than ~96% caused the sample to flow. Each panel is the scattering intensity vs q_r. The scattering momentum q_r was oriented in the plane of the multilayers. The scattering intensity is displayed in an arbitrary unit but is the same for all the panels.

These aligned samples were scanned by an X-ray along the direction normal to the substrate (Figure 2) and separately along the direction parallel to the substrate (Figure 3). Figure 2 shows the lamellar diffraction patterns of pure LPS at 25, 35, and 40 °C as the hydration level increased from 75 to ~100% RH. At 25 °C, the lamellar diffraction patterns did not change much with hydration. However, as it approached full hydration, the number of discernible orders decreased, indicating an increase in layer fluctuations. At 35 °C, the lamellar patterns at low hydration levels are similar to 25 °C. But as the hydration level increased, a second lamellar pattern with a larger Bragg angle (smaller repeat spacing) appeared, indicating that the sample entered a thermodynamic region of two coexistent phases. At 40 °C, the diffraction patterns show the same two phase coexistence as the hydration increased from 75% RH, although the second phase, the one with a smaller repeat spacing, clearly dominated particularly at high hydration levels.

This result corresponds with the wide-angle in-plane scattering shown in Figure 3. The in-plane diffraction peak at q_r (the in-plane scattering momentum) ~1.45 Å^{-1} is the well-known paraffin peak (*34*, *35*) produced by the regular distance between closely packed hydrocarbon chains. Close packing is possible only for fully saturated hydrocarbon chains, which are the case for LPS. The peak produced by LPS bilayers at low hydration levels (the first two columns in Figure 3) indicates that LPS at low hydrations is in the gel phase in which the chains were all trans and closely packed. As the hydration level exceeded ~96% RH, LPS was still in the gel phase at 30 °C, but at temperatures above 33 °C, the peak became diffuse, signaling a transition to the fluid (or liquid crystalline) state in which the chains were disordered by trans-gauche excitations.

These results showed that the gel-to-fluid transition temperatures of Rd- and Re-LPS at high levels of hydration are between 30 and 33 °C. This is in agreement with the previous measurements by Fourier transform infrared spectroscopy and differential scanning calorimetry on aqueous dispersions of Rd- and Re-LPS (*36*, *37*). Note that the gel phase extends to a higher temperature at low hydration levels.

State of LPS Bilayers. The proof of bilayers is given by the electron density profile (Figure 4, top) constructed from the lamellar diffraction amplitudes (Figure 2). The bilayer is formed by two LPS monolayers with the polar groups (that contain the high density phosphates) on the outside and the chains (low electron density) of the two monolayers facing each other in the middle, just like phospholipid bilayers (see, e.g., ref *23*). The profiles were constructed (Figure 4) from the diffraction patterns of the gel phase only since the pure fluid phase occurred near full hydration where the layer undulation fluctuations limited the diffraction to one or two peaks. Technically, it is possible to analyze the fluid phase from the coexistence region. However, it seems sufficient to conclude from the similarity of the diffraction patterns between the gel and the fluid phase that LPS maintained the bilayer form upon transition from the gel to the fluid phase. The electron density profiles of LPS containing protegrin at P/L = 1:10 are shown in Figure 4 (bottom). They are similar to pure LPS bilayers.

There is a qualitative difference between LPS multilayers and phospholipid multilayers in the degree of stacking order between bilayers. The profiles of LPS in the gel phase resemble the profiles of phospholipids (e.g., of dimyristoyl phosphatidylcholine (DMPC) in the fluid phase at hydration levels less than 98% RH (*36*)). DMPC in the gel phase has

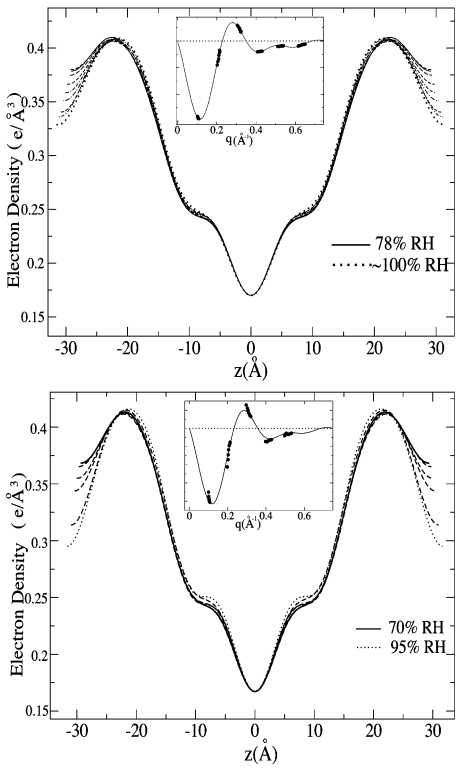

FIGURE 4: Electron density profiles of the LPS Re bilayer (top) and the LPS Re bilayer containing protegrin-1 at P/L = 1:10 (bottom) at 25 °C and at various hydration levels. The insets show the phasing diagrams, the scattering amplitude vs *q*, of the swelling method (*24*). The profiles were normalized approximately by assuming that 20 water molecules associated with each lipid and assuming that the middle of the bilayer has a density of CH_3, 0.17 e/Å^3 (*21*, *22*).

fine structures in the profile indicating a close packing of the chains as well as a high degree of stacking order between bilayers (*38*). Since the in-plane paraffin peaks (Figure 3) showed a close packing of LPS chains, the lack of fine structures in the electron density profile of gel phase LPS implies that the bulky headgroup of LPS prevents the lipids from achieving the degree of stacking order achievable by phospholipids. As a result, the number of discernible diffraction orders is reduced from 12 for DMPC in the gel phase to six for LPS in the gel phase. The resolution of the diffraction patterns for LPS in the gel phase is comparable to DMPC in the fluid phase.

Ions play important roles in the functions of LPS (*2*) and might be a factor in peptide−LPS interactions. Thus, we measured and compared the profiles of LPS bilayers with and without barium ions (barium was chosen for its large atomic number for X-ray contrast). The results are shown in Figure 5. From the difference profile (*22*), we see that barium ions are localized within a small range (∼7 Å) in the headgroup region where anionic groups are located. It is important to note that the presence of ions did not significantly affect the quality of LPS multilayers.

States of Antimicrobial Peptides Bound to LPS Bilayers. OCD has been successfully used to study the physical state of the peptides embedded in phospholipid bilayers. OCD determines not only the secondary structure of a peptide but also its orientation in membranes (*15*, *16*). The ease of OCD measurement makes it a very effective method for probing the peptide orientation in membranes, particularly if the

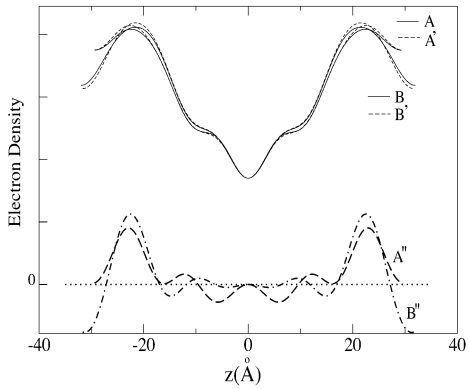

FIGURE 5: Electron density difference profiles for barium ions. Two pairs of relatively normalized electron density profiles of pure LPS Re (solid curve A and B) and LPS Re with barium ions at the lipid-to-barium molar ratio of 10:1 (dashed line A′ and B′) are shown at a low hydration level (A and A′) and at a high hydration level (B and B′). The difference profiles A″ = A′ − A (long dash) and B″ = B′ − B (dash dot) show the location of the barium ions. The scale of the difference profiles was magnified relative to the bilayer profiles.

orientation changes with membrane conditions. The simplest cases are α-helical peptides. All helical peptides we have investigated, including alamethicin (*15*−*17*, *25*, *39*, *40*), magainin (*28*), and melittin (*29*, *40*), showed two possible orientations in phospholipid bilayers, each with a distinct OCD spectrum. In general, helical peptides are bound to the bilayer with the helical axis parallel to the plane of the bilayers in low peptide concentrations (expressed as the peptide-to-lipid ratio, P/L). However, above a certain critical peptide concentration P/L* the peptides change to the perpendicular orientation. Each peptide appears to have its own unique P/L* in each lipid composition of bilayer. In a binary lipid mixture, P/L* changes continuously with the ratio of the mixture (*27*). We have also found that when peptides were oriented perpendicular to the bilayer as indicated by OCD, neutron diffraction showed transmembrane pores in the bilayers (*29*, *41*−*43*). The diffraction pattern for pores disappeared when OCD indicated that peptides were parallel to the bilayers (*29*, *42*). Thus, for helical peptides, the perpendicular orientation signifies the active state of the peptide. For the *β*-sheet peptide protegrin-1, we have also determined the OCD spectrum for its active state by the similarity of the behavior between protegrin-1 and α-helical peptide alamethicin (*31*). These results from phospholipid bilayers will now be used as a reference for our studies with LPS.

LPS is different from phospholipids in having large CD amplitudes. CD of phospholipids is at least an order of magnitude smaller than that of peptides. For example, at P/L ∼1:25, the maximum CD amplitude of pure phospholipids is 1/20 to 1/10 of the maximum CD amplitude of the peptides (*15*, *40*). As a result, the corrections for phospholipid background are relatively insignificant for P/L >1:30. On the contrary, LPS has a strong CD due to its oligosaccharide headgroup. Figure 6 shows an OCD spectrum of pure LPS multilayers, whose maximum peak amplitude is larger than the OCD of LPS containing melittin at P/L = 1:5. Thus, for every peptide sample, one has to prepare a counterpart of pure LPS with the identical amount of lipid so that the lipid background can be subtracted correctly. The strong signal of LPS makes the CD measurement difficult for low peptide

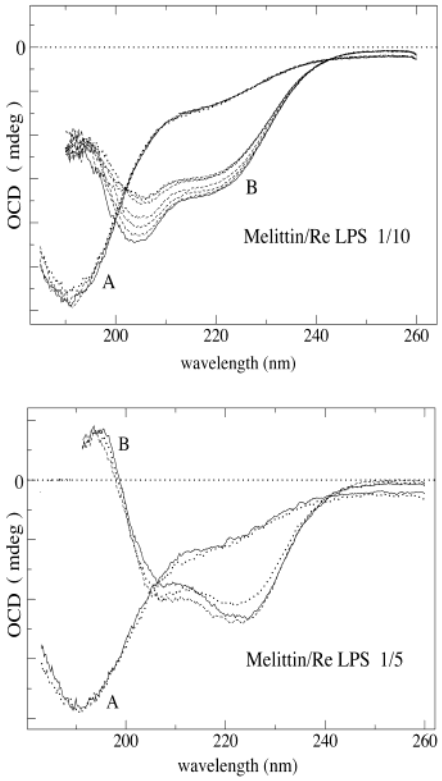

FIGURE 6: Oriented circular dichroism of LPS multilayers with and without melittin. CD spectra were taken with UV light incident normal to the plane of multilayers. Top panel: (A) OCD of pure LPS Re with the same amount of lipid as in B. (B) OCD of LPS Re containing melittin at P/L = 1:10. Both were measured at various hydration levels. The spectra of pure LPS Re were insensitive to the hydration level. The spectra of melittin in LPS Re varied somewhat with hydration: the solid curve was measured at the highest hydration level ~98% RH; the spectrum shifted upward with decreasing hydration. Bottom panel: (A) OCD of pure LPS Re with the same amount of lipid as in B. (B) OCD of LPS Re containing melittin at P/L = 1:5, at various hydration levels. The spectra were insensitive to the variation of the hydration level in both cases. The spectra of LPS containing melittin were limited to above the wavelength of 190 nm due to the strong UV absorption by the peptide. (The spectra are displayed on an arbitrary scale.)

concentrations. As we will explain below, the physiological concentrations of antimicrobial peptides are very high, corresponding to P/L ≥1:15 for LPS. Thus, we focus our measurements on peptide concentrations P/L ≥1:20.

We first tested the method of OCD in LPS with melittin because this membrane-active peptide is readily available and has been studied extensively (see ref *29* and references therein). Melittin spectra were measured as a function of P/L. (Only the spectra of P/L = 1:10 and 1:5 are shown in Figures 6 and 7.) The LPS-subtracted spectra are shown in Figure 7. The spectra were also measured at various degrees of hydration for two reasons. (1) The hydration dependence allows us to determine the correct spectrum at full hydration. (2) The physical property of lipid bilayer changes with hydration. Therefore, the hydration dependence is a simple method of probing if the peptide orientation varies with the physical property of the bilayer. We note that the OCD of pure LPS is independent of the degree of hydration (Figure 6). The OCD of melittin at P/L = 1:10 varied somewhat with hydration, but at P/L = 1:5, the spectrum did not change much with hydration.

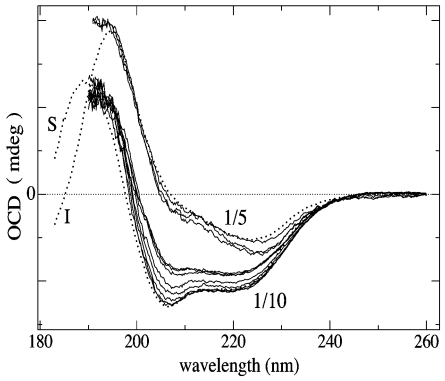

FIGURE 7: Oriented circular dichroism (OCD) of melittin in LPS bilayers at P/L = 1:10 and 1:5 and at different hydration levels were obtained by the differences (B − A) of Figure 6. The dotted lines are the OCD of melittin in phospholipid bilayers (*29*). Spectrum I is the OCD of melittin oriented perpendicular to the plane of bilayers. Spectrum S is the OCD of melittin oriented parallel to the bilayers. Melittin in LPS at P/L = 1:5 has the spectrum I, independent of hydration level. Melittin in LPS at P/L = 1:10 has the spectrum S at the highest hydration level. At the lower hydration levels, each spectrum is a linear superposition of spectrums I and S. As the hydration level decreased, a small but increasing fraction of melittin molecules is in spectrum I. Note that the spectra I and S are relatively normalized to each other since they were obtained from one sample (*29*) but not normalized to an absolute scale. The spectra from LPS were multiplied by a factor to match the amplitudes of S and I, respectively.

The OCD spectra of α-helical peptides are well-understood theoretically (refs *15* and *16* and references therein). We know that the OCD spectrum of P/L = 1:10 measured at full hydration (Figure 7) is the CD of helices oriented perpendicular to the incident light or parallel to the membranes (denoted as the S spectrum for the surface state; its difference from the solution CD was explained in ref *16*). The same OCD was obtained from melittin in DMPC at the condition that melittin was parallel to the phospholipid bilayers (*29*). On the other hand, the OCD at P/L = 1:5 is the CD of helices oriented parallel to the incident light or perpendicular to the membranes (denoted as the I spectrum for the insertion state), characterized by the vanishing amplitude of the negative peak at ~205 nm (*15*, *16*). Again, the same OCD was also obtained from melittin in DMPC at the condition that melittin was perpendicular to the lipid bilayers. We will not discuss the hydration dependence of the OCD here, except to note that the OCD of P/L = 1:10 measured at less than full hydration is a linear combination of the two basis spectra; one represents parallel and another perpendicular orientations. At peptide concentrations below P/L = 1:10, the melittin spectra are the same as at P/L = 1:10 (i.e., the helical axis is parallel to the plane of LPS bilayers). This orientation dependence on P/L (i.e., parallel to the membrane at low P/L's and perpendicular to the membrane at high P/L's) is similar to the behavior of melittin in phospholipid bilayers (*29*, *40*). The fact that the OCD spectra of melittin in LPS are identical to those obtained from melittin in phospholipids (*29*) proved that OCD can be used for LPS studies.

Encouraged by the result of melittin, we proceeded to measure the OCD of two representative antimicrobial peptides: the helical peptide magainin and the β-sheet peptide protegrin. The OCD spectra of magainin-2 in fully hydrated LPS are shown in Figure 8. These OCD spectra are the same

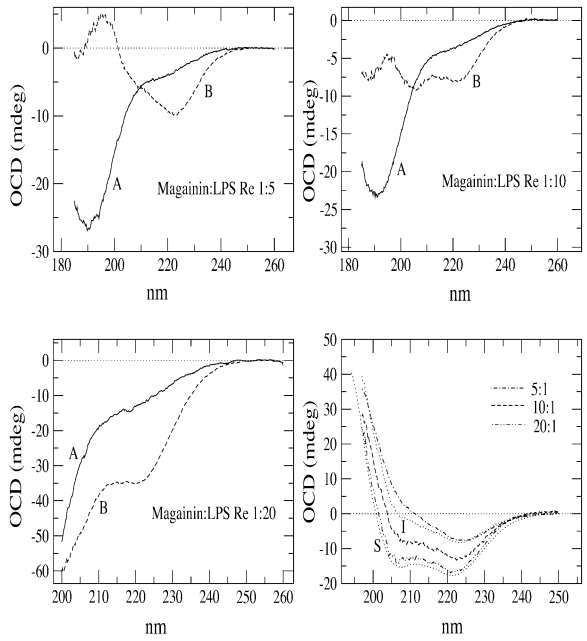

FIGURE 8: OCD of magainin in LPS. The spectra were obtained in the same manner as in Figures 6 and 7. The spectra of magainin showed little hydration dependence, so only one spectrum is shown for each P/L. The right bottom panel shows the LPS-subtracted magainin spectra. The dotted lines are the OCD of magainin in phospholipid bilayers (*28*), where I is the OCD of magainin oriented perpendicular to the bilayer, and S is the OCD of magainin oriented parallel to the bilayers.

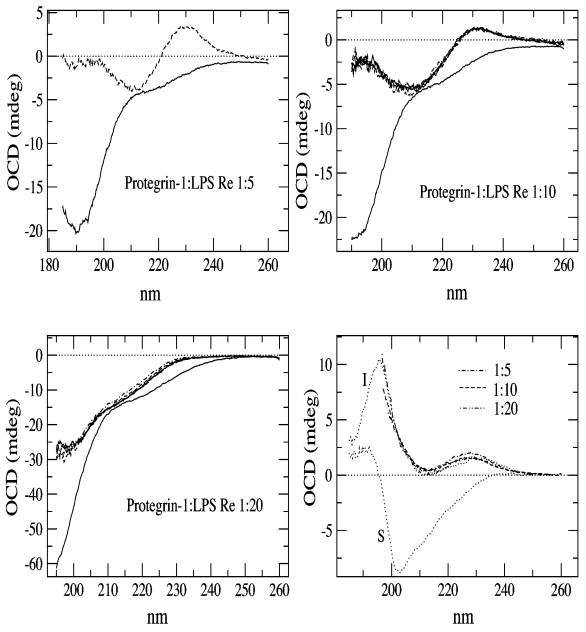

FIGURE 9: OCD of protegrin in LPS. The spectra were obtained in the same manner as in Figures 6 and 7. The spectra of protegrin showed little hydration dependence, so only one spectrum is shown for each P/L. The right bottom panel shows the LPS-subtracted protegrin spectra. The dotted lines are the OCD of protegrin in phospholipid bilayers (*31*), where I is the OCD of protegrin in the active state, and S is the OCD of protegrin in the inactive state (see ref *31* for details).

as obtained from magainin in phospholipid bilayers (*28*). The results are summarized as follows: below P/L = 1:20, magainin peptides bind to LPS bilayers with the helical axis parallel the plane of the bilayers; above P/L = 1:10, the peptides are oriented perpendicular to the bilayers.

The OCD spectra of β-sheet peptide protegrin-1 were measured in the same manner (Figure 9). Because the CD spectra of β-sheet peptides are not understood theoretically, their interpretation relies on a comparison with α-helical peptides. In a very detailed comparison of protegrin and alamethicin (*31*), we have identified the spectrum shown in Figure 9 as the active state of protegrin-1, corresponding to alamethicin oriented perpendicular to the membranes. Protegrin-1 has another OCD corresponding to alamethicin oriented parallel to the membranes (*31*). This spectrum did not show up in the LPS samples for P/L ≥1:20.

Because of the importance of ions to the functions of LPS (*2*), we examined the effects of monovalent ions and divalent ions on the orientation of peptides in LPS bilayers. Very high salt concentrations (expressed in the ion-to-lipid molar ratio, I/L) in the chloride and acetate forms were incorporated in the LPS preparations, including Ca^{2+}, Mg^{2+}, and Na^{+} at I/L = 1:10 and 1:5. The OCD of antimicrobial peptides in LPS varied slightly with these salts, but the changes were insignificant. We also repeated the measurements at different temperatures, 25, 35, and 40°. The orientation of antimicrobial peptides remains essentially the same within this range of temperature.

CONCLUSION

Despite the complex structure of the LPS molecule, its bilayer structure is surprisingly similar to that of phospholipids. In the gel phase, the chains of LPS are all trans and closely packed. However, the complex structures of the oligosaccharide region prevent the multilayers from achieving a stacking order comparable to that of phospholipids. In the fluid phase, the diffraction patterns of pure LPS consist of only a few Bragg orders, insufficient for structural analysis. However, when LPS bilayers include peptides, the diffraction patterns changed slowly and systematically with hydration (similar to the case for dilauroyl phosphatidylcholine or DLPC containing gramicidin—see ref *22*). In the presence of a high concentration of peptides, the lipid chains are always disordered; there is no chain-melting transition from a fluid phase to a well-ordered gel phase. Thus, it is possible to study the electron density profile of peptide-containing LPS bilayers in somewhat dehydrated states, where six Bragg orders have been observed.

The OCD of melittin, magainin, and protegrin in LPS reproduced the spectra measured in phospholipids. In phospholipids, the most striking results of OCD studies were that the peptide orientation depends on both the peptide concentration and the lipid composition of the bilayers. The transition of the peptide orientation takes place over a small range of P/L. Below a threshold P/L*, the peptide is embedded in the headgroup region of the membrane, but above P/L*, the peptide is transmembrane (see references in ref *9*). For example, the melittin threshold P/L* is very low in phospholipids with unbranched, saturated chains, such as DMPC and DLPC—in fact, the thresholds were too low (P/L* <1:300) to be detected. The melittin thresholds in phospholipids with branched chains, such as diphytanoyl phosphatidylcholine (DPhPC), or with unsaturated chains, such as dioleoyl phosphadylcholine (DOPC) and palmitoyloleoyl phosphatidylcholine (POPC), are higher, usually P/L >1:100 (*29*, *40*). This difference in P/L* can be understood qualitatively in terms of the areal ratio of the lipid headgroup

to the chains A_{hg}/A_{ch} (*27*) (e.g., the ratio for POPC is smaller than that for DMPC). A smaller A_{hg}/A_{ch} can accommodate more peptides in the headgroup region, before the membrane thinning effect causing the peptide to change to the transmembrane orientation (*27*, *39*, *40*), hence a higher P/L*. Similarly, P/L* of magainin is below 1:30 in DMPC and higher than 1:20 in POPC (*28*, *43*). P/L* of protegrin is below 1:100 in DMPC and is ~1:60 in DPhPC (*31*). It is quite unexpected to find that in a complex lipid like LPS there is also a sharp threshold P/L* for the change of peptide orientation. Furthermore, since all the chains of LPS are unbranched and saturated, one would expect a low threshold concentration. But, surprisingly, the thresholds for melittin and magainin in LPS are between 1:10 and 1:5 (corresponding to 1:30 < P/L* < 1:15 in phospholipids, in view of the fact that each LPS has six or seven chains).

The physiological concentrations of antimicrobial peptides were estimated by Merrifield's group in a series of radioactivity binding experiments (*44*, *45*). They found that with different bacteria of different size and shape, the amount of peptide required for lysis was roughly equivalent to the amount needed for forming a monolayer around that bacterium. In terms of the peptide-to-lipid molar ratio, this is in the order of P/L ~1:5−1:10. This estimate agreed with subsequent experiments (e.g., refs *46* and *47* for protegrin). At such high concentrations, both magainin and protegrin readily penetrate LPS bilayers. This suggests the possibility that the peptides might also penetrate the outer membranes.

In physiological conditions, the peptides bound to the outer membrane are initially in kinetic equilibrium with the extracellular peptides. Once the peptides penetrate the outer membrane, the periplasmic space and the inner membrane become accessible to the peptides. The peptide distribution will then approach a new partition among four populations (i.e., those in the extracellular and periplasmic solutions and those bound to the two membranes). Experiments with phospholipid bilayers suggest that antimicrobial peptides form a high density of pores in the plasma membrane if a sufficient amount of peptides permeate through the outer membrane (*9*).

REFERENCES

1. Nikaido, H. (1994) Prevention of drug access to bacterial targets: permeability barriers and active efflux, *Science 264*, 382−388.
2. Nikaido, H. (1999) Outer membrane in *Escherichia coli and Salmonella typhimurium* (Neidhardt, F. C., Ed.) Vol. 1, pp 29−47, American Society for Microbiology, Washington, DC.
3. Snyder, D. S., and McIntosh, T. J. (2000) The lipopolysaccharide barrier: correlation of antibiotic susceptibility with antibiotic permeability and fluorescent probe binding kinetics, *Biochemistry 39*, 11777−11787.
4. Martin, E., Ganz, T., and Lehrer, R. I. (1995) Defensins and other endogenous peptide antibiotics of vertebrates, *J. Leukocyte Biol. 58*, 128−136.
5. Ganz, T. (1999) Defensins and host defense, *Science 286*, 420−421.
6. Ganz, T. (2000) Paneth cells−guardians of the gut cell hatchery, *Nat. Immunol. 2*, 99−100.
7. Boman, H. G., Marsh, J., and Goode, J. A., Eds. (1994) *Antimicrobial Peptides*, Ciba Foundation Symposium 186, pp 1−272, John Wiley & Sons, Chichester.
8. Matsuzaki, K. (1998) Magainins as paradigm for the mode of action of pore forming polypeptides, *Biochim. Biophys. Acta 1376*, 391−400.
9. Huang, H. W. (2000) Action of antimicrobial peptides: Two-state model, *Biochemistry 39*, 8347−8352.
10. Negrete, H. O., Rivers, R. L., Gough, A. H., Colombini, M., and Zeidel, M. L. (1996) Individual leaflets of a membrane bilayer can independently regulate permeability, *J. Biol. Chem. 271*, 11627−11630.
11. Hill, W. G., Rivers, R. L., and Zeidel, M. L. (1999) Role of leaflet asymmetry in the permeability of model biological membranes to protons, solutes, and gases, *J. Gen. Physiol. 114*, 405−414.
12. Labischinski, H., Barnickel, G., Bradaczek, H., Naumann, D., Rietschel, E. T., and Giesbrecht, P. (1985) High state of order of isolated bacterial lipopolysaccharide and its possible contribution to the permeation barrier property of the outer membrane, *J. Bacteriol. 162*, 9−20.
13. Kastowsky, M., Gutberlet, T., and Bradaczek, H. (1993) Comparison of X-ray powder diffraction data of various bacterial lipopolysaccharide structures with theoretical model conformations, *Eur. J. Biochem. 217*, 771−779.
14. Snyder, S., Dennis, K., and McIntosh, T. J. (1999) Lipopolysaccharide bilayer structure: effect of chemotype, core mutations, divalent cations, and temperature, *Biochemistry 38*, 10758−10767.
15. Olah, G. A., and Huang, H. W. (1988) Circular dichroism of oriented α-helices. I. Proof of the exciton theory, *J. Chem. Phys. 89*, 2531−2538.
16. Wu, Y., Huang, H. W., and Olah, G. A. (1990) Method of oriented circular dichroism, *Biophys. J. 57*, 797−806.
17. Huang, H. W., and Wu, Y. (1991) Lipid−alamethicin interactions influence alamethicin orientation, *Biophys. J. 60*, 1079−1087.
18. Zasloff, M. (1987) Magainins, a class of antimicrobial peptides from *Xenopus* skin: Isolation, characterization of two active forms, and partial cDNA sequence of a precursor, *Proc. Natl. Acad. Sci. U.S.A. 84*, 5449−5453.
19. Kokryakov, V. N., Harwig, S. S. L., Panyutich, E. A., Shevchenko, A. A., Aleshina, G. M., Shamova, O. V., Korneva, H. A., and Lehrer, R. I. (1993) Protegrins: leukocyte antimicrobial peptides that combine features of corticostatic defensins and tachyplesins, *FEBS Lett. 327*, 231−236.
20. Yang, L., Weiss, T. M., Lehrer, R. I., and Huang, H. W. (2000) Crystallization of antimicrobial pores in membranes: magainin and protegrin, *Biophys. J. 79*, 2002−2009.
21. Wu, Y., He, K., Ludtke, S. J., and Huang, H. W. (1995) X-ray diffraction study of lipid bilayer membrane interacting with amphiphilic helical peptides: diphytanoyl phosphatidylcholine with alamethicin at low concentrations, *Biophys. J. 68*, 2361−2369.
22. Olah, G. A., Huang, H. W., Liu, W., and Wu, Y. (1991) Location of ion binding sites in the gramicidin channel by X-ray diffraction, *J. Mol. Biol. 218*, 847−858.
23. Chen, F. Y., Hung, W. C., and Huang, H. W. (1997) Critical swelling of phospholipid bilayers, *Phys. Rev. Lett. 79*, 4026−4029.
24. Blaurock, A. E. (1971) Structure of the nerve myelin membrane: proof of the low resolution profile, *J. Mol. Biol. 56*, 35−52.
25. Harroun, T. A., Heller, W. T., Weiss, T. M., Yang, L., and Huang, H. W. (1999) Experimental evidence of hydrophobic matching and membrane-mediated interactions in lipid bilayers containing gramicidin, *Biophys. J. 76*, 937−945.
26. Yang, L., Harroun, T. A., Heller, W. T., Weiss, T. M., and Huang, H. W. (1998) Neutron off-plane scattering of aligned membranes I: Method of measurement, *Biophys. J. 75*, 641−645.
27. Heller, W. T., He, K., Ludtke, S. J., Harroun, T. A., and Huang, H. W. (1997) Effect of changing the size of lipid headgroup on peptide insertion into membranes, *Biophys. J. 73*, 239−244.
28. Ludtke, S. J., He, K., Wu, Y., and Huang, H. W. (1994) Cooperative membrane insertion of magainin correlated with its cytolytic activity, *Biochim. Biophys. Acta 1190*, 181−184.
29. Yang, L., Harroun, T. A., Weiss, T. M., Ding, L., and Huang, H. W. (2001) Barrel-stave model or toroidal model? A case study on melittin pores, *Biophys. J. 81*, 1475−1485.
30. Weiss, T. M., van der Wel, P. C. A., Killian, J. A., Koeppe, R. E., II, and Huang, H. W. (2003) Hydrophobic mismatch between helices and lipid bilayers, *Biophys. J. 84*, 379−385.
31. Heller, W. T., Waring, A. J., Lehrer, R. I., and Huang, H. W. (1998) Multiple states of β-sheet peptide protegrin in lipid bilayers, *Biochemistry 37*, 17331−17338.
32. Weiss, T. M., Yang, L., Ding, L., Waring, A. J., Lehrer, R. I., and Huang, H. W. (2002) Two states of cyclic antimicrobial peptide RTD-1 in lipid bilayers, *Biochemistry 41*, 10070−10076.

33. Yang, L., Weiss, T. M., Harroun, T. A., Heller, W. T., and Huang, H. W. (1999) Supramolecular structures of peptide assemblies in membranes by neutron off-plane scattering: method of analysis, *Biophys. J. 77*, 2648−2656.
34. Warren, B. E. (1933) X-ray diffraction in long chain liquids, *Phys. Rev. 44*, 969−973.
35. Luzatti, V. (968) X-ray diffraction studies of lipid−water systems, in *Biological Membranes* (Chapman, D., Ed.) pp 71−124, Academic Press, New York.
36. Brandenburg, K., and Seydel, U. (1990) Investigation into the fluidity of lipopolysaccharide and free lipid A membrane systems by Fourier transform infrared spectroscopy and differential scanning calorimetry, *Eur. J. Biochem. 191*, 229−236.
37. Seydel, U., Koch, M. H. J., and Brandenburg, K. (1993) Structural polymorphisms of rough mutant lipopolysaccharides Rd to Ra from *Salmonella minnesota*, *J. Struct. Biol. 110*, 232−243.
38. Hung, W. C., Chen, F. Y., and Huang, H. W. (2000) Order−disorder transition in bilayers of diphytanoyl phosphatidylcholine, *Biochim. Biophys. Acta 1467*, 198−206.
39. Chen, F. Y., Lee, M. T., and Huang, H. W. (2002) Sigmoidal concentration dependence of antimicrobial peptide activities: a case study on alamethicin, *Biophys. J. 82*, 908−914.
40. Chen, F. Y., Lee, M. T., and Huang, H. W. (2003) Evidence for a membrane thinning effect as the mechanism for peptide-induced pore formation, *Biophys. J. 84*, 3751−3758.
41. He, K., Ludtke, S. J., Worcester, D. L., and Huang, H. W. (1995) Antimicrobial peptide pores in membranes detected by neutron in-plane scattering, *Biochemistry 34*, 16764−16769.
42. He, K., Ludtke, S. J., Worcester, D. L., and Huang, H. W. (1996) Neutron scattering in the plane of membranes: structure of alamethicin pores, *Biophys. J. 70*, 2659−2666.
43. Ludtke, S. J., He, K., Heller, W. T., Harroun, T. A., Yang, L., and Huang, H. W. (1996) Membrane pores induced by magainin, *Biochemistry 35*, 13723−13728.
44. Steiner, H., Andreu, D., and Merrifield, R. B. (1988) Binding and action of cecropin and cecropin analogues: antibacterial peptides from insects, *Biochim. Biophys. Acta 939*, 260−266.
45. Merrifield, R. B., Merrifield, E. L., Juvvadi, P., Andreu, D., and Boman, H. G. (1994) in *Antimicrobial Peptides* (Boman, H. G., Marsh, J., and Goode, J. A., Eds.) Ciba Foundation Symposium 186, pp 5−26, John Wiley & Sons, Chichester.
46. Shi, J., and Ganz, T. (1998) The role of protegrins and other elastase-activated polypeptides in the bactericidal properties of porcine inflammatory fluids, *Infect. Immun. 66*, 3611−3617.
47. Albrecht, M. T., Wang, W., Shamova, O., Lehrer, R. I., and Schiller, N. L. (2002) Binding of protegrin-1 to *Pseudomonas aeruginosa* and *Burkholderia cepacia*, *Respir. Res. 14*, 18.

BI035130+